Nonintegral stoichiometry in CFTR gating revealed by a pore-lining mutation

Kang-Yang Jih,[1,2] Yoshiro Sohma,[3] and Tzyh-Chang Hwang[1,2]

[1]Dalton Cardiovascular Research Center and [2]Department of Medical Pharmacology and Physiology, University of Missouri-Columbia, Columbia, MO 65211

[3]Department of Pharmacology, Keio University School of Medicine, Shinjuku, Tokyo 160-8582, Japan

Cystic fibrosis transmembrane conductance regulator (CFTR) is a unique member of the ATP-binding cassette (ABC) protein superfamily. Unlike most other ABC proteins that function as active transporters, CFTR is an ATP-gated chloride channel. The opening of CFTR's gate is associated with ATP-induced dimerization of its two nucleotide-binding domains (NBD1 and NBD2), whereas gate closure is facilitated by ATP hydrolysis-triggered partial separation of the NBDs. This generally held theme of CFTR gating—a strict coupling between the ATP hydrolysis cycle and the gating cycle—is put to the test by our recent finding of a short-lived, post-hydrolytic state that can bind ATP and reenter the ATP-induced original open state. We accidentally found a mutant CFTR channel that exhibits two distinct open conductance states, the smaller O1 state and the larger O2 state. In the presence of ATP, the transition between the two states follows a preferred O1→O2 order, a telltale sign of a violation of microscopic reversibility, hence demanding an external energy input likely from ATP hydrolysis, as such preferred gating transition was abolished in a hydrolysis-deficient mutant. Interestingly, we also observed a considerable amount of opening events that contain more than one O1→O2 transition, indicating that more than one ATP molecule may be hydrolyzed within an opening burst. We thus conclude a nonintegral stoichiometry between the gating cycle and ATP consumption. Our results lead to a six-state gating model conforming to the classical allosteric mechanism: both NBDs and transmembrane domains hold a certain degree of autonomy, whereas the conformational change in one domain will facilitate the conformational change in the other domain.

INTRODUCTION

CFTR is a unique member of the ATP-binding cassette (ABC) protein superfamily because although most members in this family are active transporters, CFTR is a bona fide ion channel. Despite this functional disparity, the overall architecture of CFTR seems well conserved. Canonical domains that a typical ABC transporter is made of, namely two transmembrane domains (TMDs), each conjoined to a nucleotide-binding domain (NBD), are clearly preserved in CFTR. Recent published structures of CFTR's two NBDs reveal almost identical structural motifs seen in all ABC proteins (Lewis et al., 2004; Dawson and Locher, 2006; Hollenstein et al., 2007; Aller et al., 2009; and Protein Data Bank accession no. 3GD7). Furthermore, functional studies in the past decade have provided evidence that the operational mechanism of CFTR shares strikingly similar features to at least the exporter members of the ABC protein family. For example, gating of CFTR is controlled by ATP binding and hydrolysis that induce, respectively, association and dissociation of the two NBDs (Vergani et al., 2005), a central theme that operates in all ABC proteins. Upon ATP binding, CFTR's NBD2 undergoes an induced-fit conformational change (Szollosi et al., 2010) that has also been proposed for ABC transporters based on comparison between the ATP-bound and ATP-free crystal structures of individual NBD (Gaudet and Wiley, 2001; Karpowich et al., 2001). Recently, Bai et al. (2010, 2011) demonstrated that CFTR uses evolutionarily conserved transmembrane segments for the construction of its ion permeation pathway, and that the conformational changes of CFTR's TMDs during gating transitions resemble what has been proposed for ABC transporters. Thus, unraveling the gating mechanism of CFTR could bear broader ramifications.

One of the most intriguing questions about CFTR is the role of ATP hydrolysis—the hallmark for an active transport process—in driving gating conformational changes. Two decades of research have gained enormous understanding about the gating mechanism of CFTR. It is now well accepted that after phosphorylation by PKA in the serine-rich regulatory domain (Gadsby et al., 1994; Bompadre et al., 2005a; Csanády et al., 2005; Mense et al., 2006), the gate of CFTR is

Correspondence to Tzyh-Chang Hwang: hwangt@health.missouri.edu

Abbreviations used in this paper: ABC, ATP-binding cassette; ABP, ATP-binding pocket; MTSET, 2-trimethylaminoethyl; NBD, nucleotide-binding domain; TMD, transmembrane domain; WT, wild type.

The Rockefeller University Press $30.00
J. Gen. Physiol. Vol. 140 No. 4 347–359
www.jgp.org/cgi/doi/10.1085/jgp.201210834

opened by NBD dimerization induced by binding of ATP to its two NBDs (Vergani et al., 2003, 2005; Zhou et al., 2006). An updated ATP-dependent gating model of CFTR is presented in Fig. 1. In brief, after ATP is hydrolyzed in the hydrolysis-competent site (ATP-binding pocket [ABP]2), the channel sojourns into a closed state (C2 state) with its NBDs in a partial dimeric configuration (Tsai et al., 2009, 2010b; Szollosi et al., 2011), in which the head of NBD1 and the tail of NBD2 (i.e., the catalysis-inert ABP1) remain associated with one ATP sandwiched in between while the catalysis-active ABP2 is separated and vacated. This C2 state has a dwell time of ~30 s before entering the C1 state in which the NBD dimer completely separates and the remaining ATP dissociates (Tsai et al., 2010b). As the role of each ATP-binding site and how ATP triggers the conformational change of NBDs become well understood, one of the lingering puzzles in CFTR gating is: how are the gating signals originated in the NBDs transmitted to the TMDs to control the gate, or in other words, how do NBDs and TMDs communicate during gating?

Supported by crystal structures and computer simulations (Ivetac et al., 2007; Khare et al., 2009), the popular rigid body hypothesis dictates a concurrent movement of each NBD–TMD complex during the transport cycle of ABC transporters. One functional implication of the rigid body movement hypothesis for CFTR is a strict coupling between NBDs and TMDs with a one-to-one stoichiometry between the ATP hydrolysis cycle and the gating cycle. This strict coupling hypothesis has been proposed more than a decade ago in the CFTR field and is supported by many studies. For example, the drastic effect of nonhydrolyzable ATP analogues or mutations (e.g., E1371S or K1250A) that abolish ATP hydrolysis on the open time supports the notion that ATP hydrolysis is coupled to channel closure (Gunderson and Kopito, 1994; Hwang et al., 1994; Carson et al., 1995; Vergani et al., 2003; Bompadre et al., 2005b). An asymmetrical transition between gating states suggests that the gating cycle of CFTR is driven by ATP hydrolysis (Gunderson and Kopito, 1995). Recently, microscopic kinetic analysis that shows a paucity of short-lived opening events in the open-time histogram further reinforces the strict coupling hypothesis (Csanády et al., 2010). However, in our latest report (Jih et al., 2012), by identifying a transient post-hydrolytic state (state X in Fig. 1) that is capable of voyaging into the prehydrolytic open state in response to ATP (X→X′→O1 in Fig. 1), we raised the possibility that the movement of NBDs and the opening/closing of the gate may not be synchronized. As described in Jih et al. (2012), the critical piece of experimental evidence that will contest the strict coupling hypothesis is to affirm the existence of more than one round of ATP hydrolysis within an opening burst. To do so, it is crucial to find a tool that allows real-time observation of ATP hydrolysis.

A recent fortuitous discovery provides us an opportunity to do just that. When mutating the positively charged arginine at position 352 (located in the sixth transmembrane segment, TM6) to cysteine, the mutant channel (R352C-CFTR) features two distinct open states with unequal conductance (Bai et al., 2010; compare Cui et al., 2008). Carefully scrutinizing single-channel recordings revealed a striking phenomenon: the appearance of these two open states follows a preferred order similar to that reported 17 years ago for wild-type (WT)-CFTR by Gunderson and Kopito (1995). In the presence of ATP, most often the channel leaves the closed state to enter a small conductance open state (named O1 state hereafter); however, the channel often returns to the closed state from a large conductance

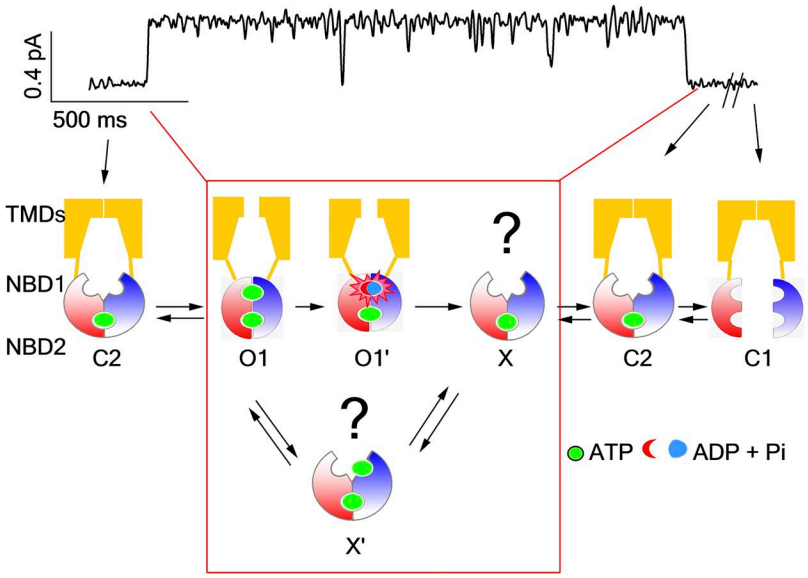

Figure 1. An updated model illustrating the relationship between an opening/closing cycle of the gate and ATP consumption in CFTR' s NBDs. The trace on top represents an opening burst of WT-CFTR. The cartoon below shows transitions of gating states throughout the gating cycle. Notably, the C2 state is extremely stable and can last for ~30 s before returning to the C1 state (Tsai et al., 2010b). C1, closed state with two separated NBDs; C2, partial NBD dimeric closed state; O1, prehydrolytic open state; O1′, post-hydrolytic open state with a full NBD dimer; X, the state with partial separated NBD dimer (Jih et al., 2012); X′, one ATP bound to the vacant ABP2 in state X. The red box encompasses the reentry pathway that may occur within each opening burst. This figure is adapted from Jih et al. (2012).

open state (named O2 state hereafter). After sorting all the opening events, we observed a dominant population that features a C→O1→O2→C transition (Table 1), whereas very rare C→O2→O1→C transitions were seen in our recordings. Such asymmetry indicates that these three states are not at thermodynamic equilibrium (Richard and Miller, 1990; Gunderson and Kopito, 1995). Instead, an input of free energy, likely coming from ATP hydrolysis, maintains these transitions at a steady state. Consistent with this idea, ATP only induces C→O1→C transitions in E1371S/R352C-CFTR, a hydrolysis-deficient mutant. The R352C mutant channel becomes a precious tool, as it allows us to distinguish the prehydrolytic (O1) and post-hydrolytic (O2) open states and thus to "visualize" ATP hydrolysis taking place within each opening burst. Interestingly, we observed opening bursts that include more than one O1→O2 transition, implicating that hydrolysis of more than one ATP molecule can take place within an opening burst. Furthermore, the frequency of opening bursts that undergo multiple rounds of ATP hydrolysis can be modulated by changing [ATP], maneuvers that greatly enhance ATP-independent opening, or introducing mutation that affects ATP binding to ABP1. Based on these results, we propose a six-state model for CFTR gating that features an energetic coupling between the NBDs and the TMDs (details are elaborated in Discussion).

MATERIALS AND METHODS

Cell culture and transient expression system

Chinese hamster ovary (CHO) cells were cultured at 37°C in Dulbecco's modified Eagle's medium supplemented with 10% fetal bovine serum. The cells were trypsinized and cultured in 35-mm tissue culture dishes 1 d before the transfection. The cDNA of CFTR and pEGFP-C3 (Takara Bio Inc.), which encodes green fluorescence protein, were cotransfected into CHO cells using PolyFect transfection reagent (QIAGEN). The cells for electrophysiological experiments were grown at 27°C for 2 d after transfection.

Mutagenesis

QuikChange XL kit (Agilent Technologies) was used according to the manufacturer's protocols to construct all the mutations used in this study. The DNA constructs were sequenced to confirm the mutation (DNA core; University of Missouri) made on cDNA.

Electrophysiological recordings

Glass chips carrying the transfected cells were transferred to a chamber located on the stage of an inverted microscope (IX51; Olympus). All the electrophysiological data were recorded at room temperature with an amplifier (EPC10; HEKA). Borosilicate capillary glasses were used to produce pipettes by using a Flaming/Brown-type micropipette puller (P97; Sutter Instrument). The pipettes were polished with a homemade microforge before experiments. In the bath solution, the resistance of pipettes for patch-clamp experiments was 2–4 MΩ. When the seal resistance was >40 GΩ, membrane patches were excised into an inside-out mode. After excision, 25 IU PKA and 2.75 mM ATP were perfused to the pipette until the CFTR current reached a steady state. 10 IU PKA was added to all other ATP-containing solutions applied thereafter to maintain the phosphorylation level. The membrane potential was held at −60 mV during recording unless specified. The data were filtered with an eight-pole Bessel filter (LPF-8; Warner Instruments) with a 100-Hz cutoff frequency and digitized to a computer at a sampling rate of 500 Hz. For a better visual effect of our data presentation, the recorded inward current was inverted. All inside-out patch experiments were performed with a fast solution exchange perfusion system (SF-77B; Warner Instruments). The dead time of solution change is ∼30 ms (Tsai et al., 2009).

Chemicals and solution compositions

The 150-mM Cl^- pipette solution contained (in mM): 140 methyl-D-glucamine chloride (NMDG-Cl), 2 $MgCl_2$, 5 $CaCl_2$, and 10 HEPES, pH 7.4 with NMDG. The 375-mM Cl^- pipette solution contained (in mM): 360 methyl-D-glucamine chloride (NMDG-Cl), 2 $MgCl_2$, 5 $CaCl_2$, and 10 HEPES, pH 7.4 with NMDG. Cells were perfused with a bath solution containing (in mM): 145 NaCl, 5 KCl, 2 $MgCl_2$, 1 $CaCl_2$, 5 glucose, 5 HEPES, and 20 sucrose, pH 7.4 with NaOH. For inside-out configuration, the 150-mM Cl^- perfusion solution contained (in mM) 150 NMDG-Cl, 2 $MgCl_2$, 10 EGTA, and 8 Tris, pH 7.4 with NMDG, and the 375-mM Cl^- perfusion solution contained (in mM) 375 NMDG-Cl, 2 $MgCl_2$, 10 EGTA, and 8 Tris, pH 7.4 with NMDG.

MgATP, DTT, and PKA were purchased from Sigma-Aldrich. MgATP and DTT were stored in 250- and 100-mM stock solution, respectively, at −20°C. 2-trimethylaminoethyl (MTSET) was purchased from Toronto Research Chemicals Inc. MTSET was stored in 100-mM stock solution at −70°C and was diluted to working concentration immediately before use. All chemicals were diluted to the concentration indicated in each figure using perfusion solution, and the pH was adjusted to 7.4 with NMDG.

Data analysis and statistics

Igor Pro program (Wavemetrics) was used to calculate the steady-state mean current amplitude and plot the histograms. Current relaxation was fitted with a single-exponential function using a Levenberg–Marquardt-based algorithm within the Igor Pro program. A program developed by Csanády (2000) was used to measure channel kinetics on traces that contain three or fewer channels. Kinetic modeling and computation simulations were described in Kopeikin et al. (2010).

Online supplemental material

Online supplemental text includes our semiquantitative analysis of the kinetic model depicted in Fig. 6. Fig. S1 shows the closed-time distribution for R352C-CFTR. Fig. S2 presents dwell-time distributions for O1 and O2 states. Fig. S3 demonstrates the effects of the W401F mutation on the single-channel kinetics of R352C-CFTR. The online supplemental material is available at http://www.jgp.org/cgi/content/full/jgp.201210834/DC1.

RESULTS

Unique pattern of single-channel gating transitions in Cysless/R352C-CFTR

During our previous studies in scanning the pore-lining residues in the sixth transmembrane segment of TMDs (TM6), a unique feature of Cysless/R352C-CFTR caught our attentions. Single-channel recordings of this CFTR mutant revealed two different open states with distinct single-channel amplitude (Fig. 2 A). However, removing the positive charge at this position also reduced the

single-channel amplitude by half, and thus the signal to noise ratio was too compromised to extract useful information about the transitions between these two conductance states from our recordings. Because this positive charge was proposed to concentrate local chloride ions in the internal vestibule of the pore (Bai et al., 2010), we reasoned that increasing [Cl^-] should overcome this technical hurdle. To our delight, elevating the chloride concentration in both the pipette and the perfusion solutions to 375 mM nearly doubled the single-channel amplitude at a −60-mV holding potential and significantly improved the signal to noise ratio (Fig. 2 B). Under such condition, two open states with distinct single-channel amplitude (O1 and O2 states, referred as the small and large conductance, respectively) can be clearly defined in the amplitude histogram (Fig. 2 B, next to each trace).

Like WT channels, this CFTR mutant opens into bursts with a lifetime of hundreds of milliseconds to seconds, and each opening burst is interrupted by very brief closures of tens of milliseconds. Close inspections of the single-channel traces reveal an interesting pattern of gating transitions: in the opening bursts that harbor both O1 and O2 states (e.g., events in red boxes in Fig. 2 B), when the channel leaves the closed state, it often opens into the smaller O1 state first, whereas when the channel returns to the closed state, it preferentially departs from the larger O2 state. Thus, the transition between O1 and O2 seems to be unidirectional, as many more C→O1→O2→C events were seen than C→O2→O1→C events (Table 1). This asymmetry in the O1↔O2 transition indicates a violation of detailed balance resulting from a free energy input that drives the gating transition in a preferred order, as first proposed

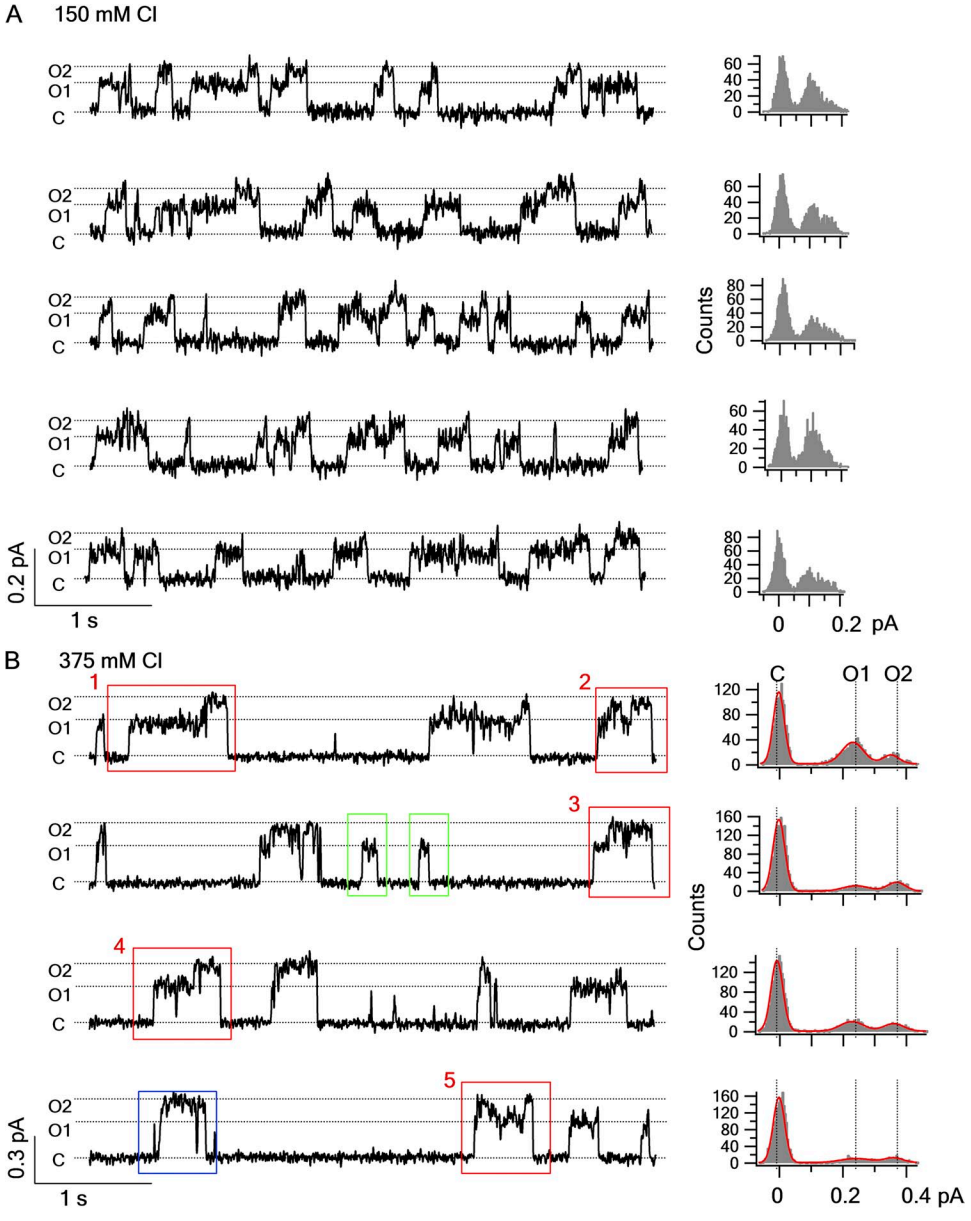

Figure 2. Cysless/R352C-CFTR reveals two different open states with distinct conductance level. (A) Five representative traces and amplitude histograms from a patch that contained only one Cysless/R352C-CFTR channel. The channel was fully phosphorylated (this also applies to Figs. 3–7), and the traces were recorded in the presence of 2.75 mM ATP. (B) Four representative traces and amplitude histograms for Cysless/R352C-CFTR recorded in a condition similar to that in A, except that both pipette and perfusion solution contain 375 mM Cl^- (see Materials and methods for details). High Cl^- solution significantly augmented the single-channel amplitude (0.17 ± 0.01 pA and n = 8 in 150 mM solutions vs. 0.38 ± 0.01 pA and n = 11 in 375 mM; holding potential = −60 mV for the larger conductance state). The events in the red boxes show a preferred order of gating transitions (i.e., C→O1→O2→C) and are expanded in Fig. 4 for clearer view. Events after the C→O1→C transition are shown in the green boxes. One event showing the C→O2→C transition is highlighted in the blue box.

for CLC-0 (Richard and Miller, 1990). Similar gating transition preference for WT-CFTR was reported by Gunderson and Kopito (1995) under a special experimental condition (see Discussion for details). For CFTR, the best candidate for the free energy source is ATP hydrolysis, as there is preponderant evidence that ATP hydrolysis fuels CFTR's gating cycle (Vergani et al., 2003; Bompadre et al., 2005b; Csanády et al., 2010). In addition, we also observed opening bursts displaying only one conductance level, i.e., C→O1→C (events in green boxes in Fig. 2 B) and C→O2→C (events in blue box in Fig. 2 B).

Notably, our results shown in Fig. 2 are somewhat different from those reported by Cui et al. (2008). They showed that in addition to O1 and O2 (named s1 and s2, respectively, in Cui et al., 2008), R352C-CFTR occasionally transits to a full conductance level that is not different from that of WT-CFTR. In four patches with ∼25 min of overall recording time, we did not observe full conductance for this mutant. The exact reason for this discrepancy remains unclear. It is possible that the full conductance state, if it exists, becomes extremely unstable in our experimental system so that those events were filtered out. Alternatively, the recordings shown in Cui et al. (2008) may actually contain more than one channel, as the mutation incidentally decreases the conductance by 50%.

ATP hydrolysis drives the O1→O2 transition

Although our initial observations were made with Cysless/R352C-CFTR, this unique pattern of gating transitions was also seen when we introduced the R352C mutation into the WT background (Fig. 3 A and Table 1). One notable difference between R352C- and Cysless/R352C-CFTR channels is that a higher percentage of C→O1→O2→C transitions were present under the WT background (Table 1). The significance of this finding will be elucidated below.

To further test our hypothesis that the dominant O1→O2 transition versus O2→O1 transition is the result of ATP hydrolysis, we engineered the E1371S mutation into R352C-CFTR to abolish ATP hydrolysis (Vergani et al., 2003; Bompadre et al., 2005b) and recorded ATP-dependent opening events. In Fig. 3 B, each of the long-lasting ATP-induced opening bursts exhibits the O1 conductance level without transiting to O2 before channel closure (Fig. 3 B). This lack of transitions to the O2 state for ATP-induced opening bursts is not caused by the mutation, E1371S, eliminating the O2 state, because in the absence of ATP, the channel opens predominantly into bursts of a larger conductance level corresponding to that of the O2 state (Fig. 3 C). Of note, in contrast to long-lived ATP-dependent openings (Fig. 3 B), these spontaneous ATP-independent openings were short-lived, with opening durations in hundreds of milliseconds (Fig. 3 C). The results presented so far bear three important implications: first, the O1→O2 transition signifies an irreversible step associated with ATP hydrolysis. Second, the C→O1 transition likely reflects openings that result from ATP-induced NBD dimerization (Vergani et al., 2005) not only because this transition dominates when ATP is present, but also because this transition is usually followed by the "hydrolysis step," O1→O2. Third, both C↔O1 and C↔O2 transitions are reversible; based on the arguments made above, we propose that the O1→C would reflect nonhydrolytic closing and C↔O2 would

TABLE 1

Summary of opening events by different gating patterns in three CFTR mutants

Gating topology	O1–O2	O1	O2	O2–O1	$(O1–O2)_n^{\#}$	Total
Cysless/R352C						
2.75 mM ATP	720 (45%)	290 (18%)	175 (11%)	42 (3%)	375 (23%)	1,602 (100%)
100 μM ATP	663 (56%)	216 (18%)	137 (12%)	32 (3%)	128 (11%)	1,176 (100%)
R352C						
2.75 mM ATP	834 (55%)	301 (20%)	173 (11%)	39 (3%)	169 (11%)	1,516 (100%)
100 μM ATP	1,246 (59%)	406 (19%)	281 (13%)	45 (2%)	121 (6%)	2,099 (100%)
R352C/W401F						
2.75 mM ATP	733 (44%)	326 (19%)	122 (7%)	28 (2%)	474 (28%)	1,683 (100%)
100 μM ATP	1,189 (54%)	367 (17%)	337 (15%)	60 (3%)	232 (11%)	2,185 (100%)

Five different gating patterns are illustrated on the top of the table. The number of events and percentage for each pattern are displayed. The corresponding CFTR mutants and ATP concentrations are shown on the left. #, the $(O1–O2)_n$ category includes events that contain at least one O2→O1 transition (such as C→O1→O2→O1→O2→C, C→O2→O1→O2→C, C→O1→O2→O1→C, C→O1→O2→O1→O2→O1→O2→C, etc.). Thus, this category in theory can be dissected into more subfamilies, but the majority of the events sorted into the $(O1–O2)_n$ category assumes a pattern of C→O1→O2→O1→O2→C, i.e., reentry occurring only one time in a burst. Because the frequency for such events is already low (∼10%), the frequency becomes even lower for opening bursts with more than one reentry event. The probabilistic nature of the distribution of these gating patterns dictates that the number of gating patterns depends on the number of event (or the duration of recordings) collected. Therefore, for simplicity, we lumped all events with more than one reentry into a single category.

represent ATP-independent spontaneous opening and closing of the gate. A simplified scheme (Scheme 1) summarizes the idea that the gating transition pattern observed in R352C-CFTR represents a cyclic steady state in which ATP hydrolysis drives a "clockwise" movement around the state diagram (compare Richard and Miller, 1990; Gunderson and Kopito, 1995).

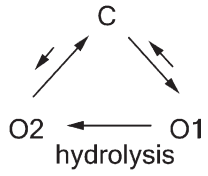

(SCHEME 1)

Non-strict coupling between ATP hydrolysis and gating cycle

If the biochemical interpretation of Scheme 1 is valid, we conclude that each C→O1→O2→C event (i.e., one gating cycle) in the single-channel recording reflects hydrolysis of one ATP molecule. Table 1 shows that for both Cysless/R352C and R352C mutant channels, C→O1→O2→C is the prevailing transition; thus, most gating events indeed follow the long-held one-to-one stoichiometry between the gating cycle and ATP hydrolysis cycle. Interestingly, however, we also found that a significant number of opening bursts contain more than one O1→O2 transition (Fig. 4 and Table 1), implying

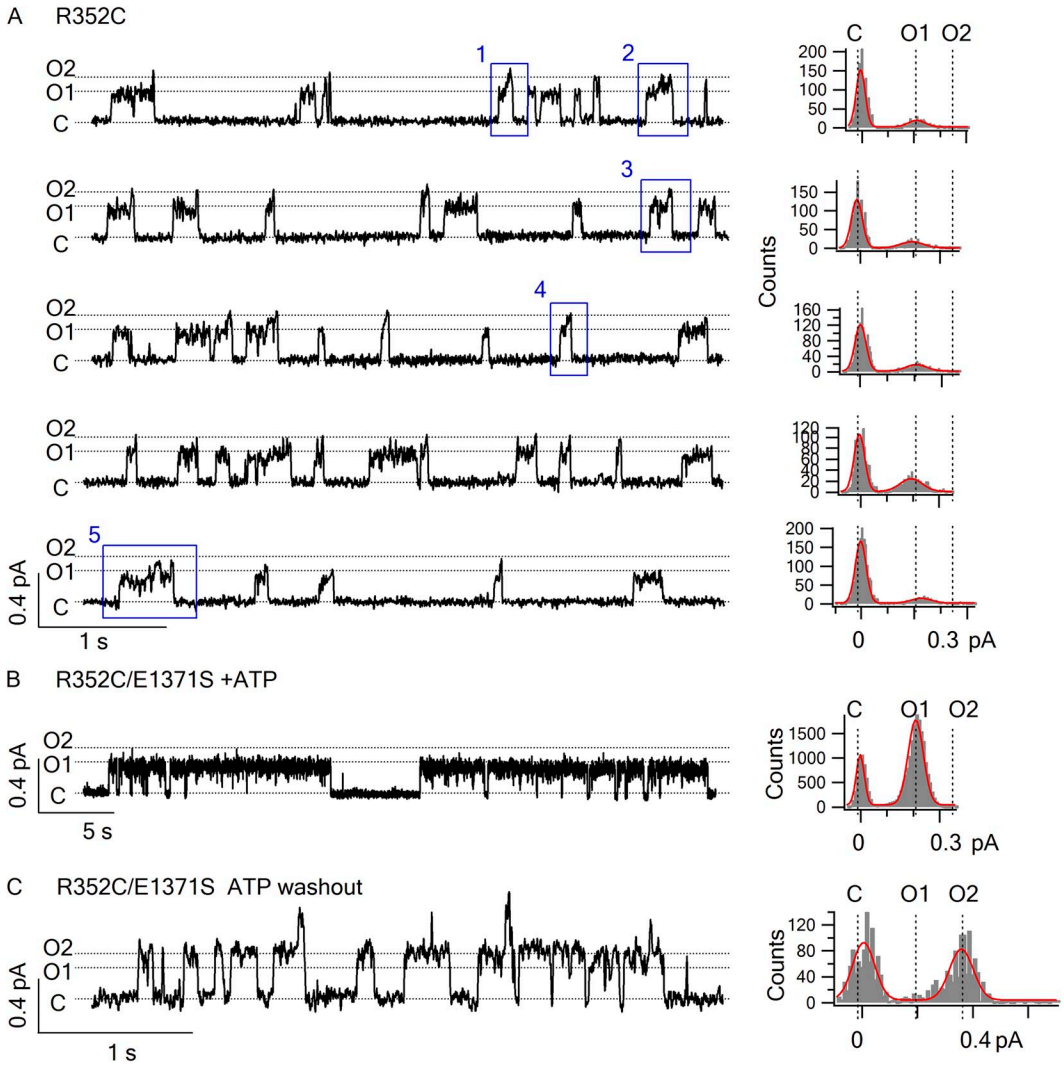

Figure 3. Hydrolysis triggers the O1→O2 transition. (A) Four representative traces and amplitude histograms show the gating pattern of R352C-CFTR channel in the presence of 2.75 mM ATP. The events in blue boxes are expanded in Fig. 4 for clearer view. (B and C) Representative traces and amplitude histograms for R352C/E1371S-CFTR in the presence (B) or absence (C) of 2.75 mM ATP. The traces were recorded in 375 mM of pipette and perfusion solution (applied to Figs. 4 and 5 as well). Similar observations were made in three patches.

that hydrolysis of more than one ATP molecule does take place within an opening burst. The existence of O2→O1 transition within an opening burst suggests that the post-hydrolytic open state (O2) can reenter the prehydrolytic O1 state before closing. Structurally, it implies that the O2 state has already had its ABP2 vacated so that it is accessible to ATP for initiating another hydrolysis cycle. This scenario predicts that the frequency of O2→O1 transitions should be [ATP] dependent. Consistent with this idea, fewer "reentry" events (i.e., O1→O2→O1→O2 transitions) were found at lower [ATP] (Table 1). Based on this finding, a new pathway is amended to Scheme 1 to illustrate the reentry events (O2→O2 ATP→O1) in the presence of ATP (Scheme 2). These two newly added kinetic steps should be reversible, as we found no reason to presume an infusion of free energy in any of them.

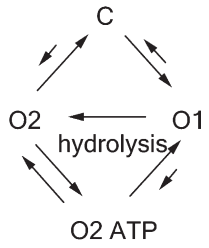

(SCHEME 2)

Before we accept this new scheme that implicates a non-strict coupling between the gating cycle and ATP hydrolysis cycle, we consider an alternative scenario that may uphold the more parsimonious theory of one-to-one stoichiometry. Because the limited bandwidth of our recordings renders events <3 ms (t_{10-90} = 0.3/filter frequency) "invisible," we cannot eliminate the possibility of the existence of a very brief closure right after each O1→O2 transition in those opening bursts presumed to embody multiple rounds of ATP hydrolysis. However, these nondiscernible closures, if they exist, are not the same as the original closed state (C in Scheme 1) for the following reasons: (a) the closed state of R352C-CFTR marked with stars in Fig. 2 assumes a very long lifetime (~1 s [Fig. S1] vs. 300–400 ms for WT-CFTR); thus, the probability of having this state with a lifetime of <3 ms buried in an opening burst is extremely small (<0.003); (b) for this idea to be valid, one has to propose that ATP can open this presumed brief closed channel at a rate that is two to three orders faster than it does to the original closed state; and (c) as shown in the next section, multiple rounds of O1→O2 transitions can take place within an opening burst in conditions when the O2 state is stabilized, a theme predicted by Scheme 2. Although more complicated schemes with additional states may explain these results, we considered Scheme 2 the simplest model (see Discussion for details).

Modulation of the reentry frequency by stabilizing the O2 state

An important implication of Scheme 2 is that the lifetime of the O2 state plays a crucial role in determining the frequency of the reentry events (i.e., opening bursts with multiple O1→O2 transitions). At a given [ATP], the longer the channel stays in the O2 state, the more likely an ATP would act to shove the channel back to the O1 state. This idea is first supported simply by comparing the Cysless/R352C- and R352C-CFTR results shown in Table 1. The Cysless/R352C mutant channel has an O2 state that is about four times as long as that in

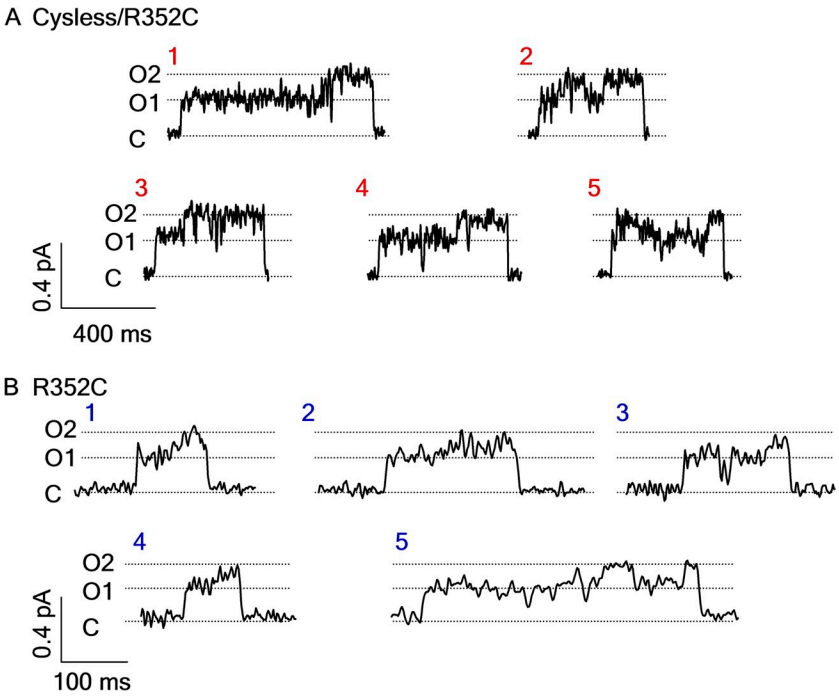

Figure 4. Non-strict coupling between ATP hydrolysis and gating cycle. Opening events of Cysless/R352C- (A) or R352C-CFTR (B) containing one (events 1, 3, and 4 in A, and 1–4 in B) or more (events 2 and 5 in A, and 5 in B) O1→O2 transitions. Events were extracted from traces in Figs. 2 B and 3 A. Chosen events were specified in boxes and numbered in Figs. 2 B and 3 A.

the R352C-CFTR (Fig. S2). Correspondingly, the percentage of opening bursts encompassing more than one O1→O2 transition is higher in Cysless/R352C (Table 1). Because the post-hydrolytic O2 state also represents spontaneous opening of the closed channel in the absence of ATP (C→O2 in Scheme 2), to further support Scheme 2, all we need here is a channel that exhibits robust ATP-independent gating.

Another serendipitous discovery in our laboratory grants us this opportunity. In Bai et al. (2010), we showed that after Cysless/I344C-CFTR is modified by MTSET, the open probability of this CFTR mutant in the presence of ATP becomes virtually 1 (Bai et al., 2010). More intriguingly, even minutes after ATP washout, the open probability remains >0.5 (compared with <0.01 for WT-CFTR; Bompadre et al., 2005b), with visibly long opening bursts. Based on Scheme 2, we predict that, when removing the positive charge at position 352 in Cysless/I344C-CFTR, these long ATP-independent openings should show up as the larger O2 state, and that, in the presence of ATP, an opening burst could contain numerous O1→O2 transitions. Fig. 5 confirms these predictions.

We introduced the R352Q mutation into the Cysless/I344C-CFTR channel. Before MESET modification, Cysless/I344C/R352Q mutant channels behaved similarly as Cysless/R352C-CFTR in the presence of ATP (Fig. 5 A). Two distinct conductance levels representing the O1 and O2 states, respectively, can be readily observed in the amplitude histogram. The preferred order of gating transition, C→O1→O2→C, as well as opening bursts with the reentry events was also preserved (expanded traces in Fig. 5 A).

After MTSET modification of Cysless/I344C/R352Q, we indeed observed robust ATP-independent openings (Fig. 5 B) with an open lifetime of 1.03 ± 0.30 s (n = 10),

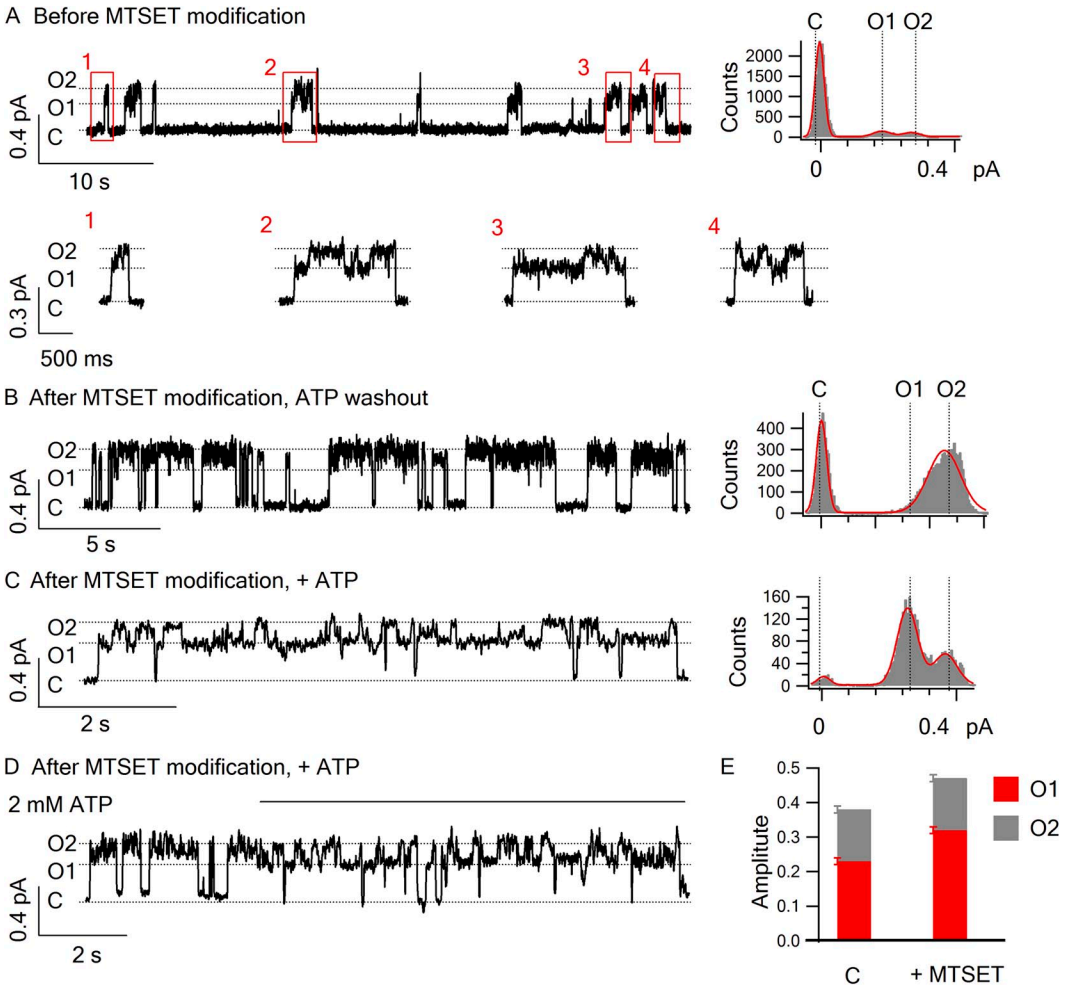

Figure 5. Modulation of the reentry frequency by stabilizing the O2 state. Representative traces and amplitude histograms for Cysless/I344C/R352Q-CFTR under these conditions: (A) in the presence of 2.75 mM ATP; (B–C) after MTSET modification, in the absence (B) or presence (C) of 2.75 mM ATP. (D) The trace highlights the O2→O1 transition when 2.75 mM ATP was applied to the patch after witnessing an ATP-independent channel opening. (E) The amplitude of O1 and O2 states of Cysless/I344C/R352Q-CFTR before (the left bar) or after (the right bar) being modified by MTSET. The O1/O2 ratio is 0.6 ± 0.02 (n = 8) before MTSET modification versus 0.68 ± 0.02 (n = 11) after MTSET modification. $P < 0.05$.

which is approximately fivefold longer than the mean lifetime of the O2 state for Cysless/R352C-CFTR (Fig. S2). In addition, the single-channel amplitude is increased by MTSET modification, an interesting yet unsurprising result because residue 344, located two helical turns extracellular to position 352, also lines the chloride permeation pathway (Bai et al., 2010). Once the patch was treated with ATP, the single-channel amplitude of the initial opening step (O1) is smaller than that of ATP-independent openings (O2). But multiple back-and-forth transitions between two levels of conductance (O1↔O2) are in display for several seconds before the opening burst is terminated into a long closure (Fig. 5 C). Of note, just like unmodified channel, there is a preference of channel closing from the large conductance state (O2). Thus, once the O2 state is stabilized, the channel is trapped in the lower half of Scheme 2, with repetitive counterclockwise cycles driven by ATP binding and hydrolysis.

To further verify the existence of the O2→O2 ATP→O1 transition depicted in Scheme 2, we applied ATP after witnessing that the ATP-independent opening occurred (Fig. 5 D). Within a second upon the application of ATP, the channel transits from the O2 state directly to the O1 state without a discernible transition to a closed state. Subsequently, in the continuous presence of ATP, multiple rounds of O1→O2→O1 transitions similar to that described in Fig. 5 C are presented. (Similar results were obtained in four patches.) These results reaffirm the idea that in the absence of ATP, the channel opens spontaneously into the post-hydrolytic O2 state, which can reenter the O1 state upon ATP binding. By comparing the single-channel amplitude before and after MTSET modification, we also noted that adding a positively charged adduct at position 344 increases the current amplitude of the O1 state slightly more than it does on the O2 state (Fig. 5 E). The significance of this finding will be discussed.

W401F mutation promotes O2→O1 transition

In our latest paper (Jih et al., 2012), using nonhydrolyzable ATP analogues (pyrophosphate or adenylyl-imidodiphosphate) as baits, we captured a post-hydrolytic state (state X), which, like the O2 state in this paper, can reenter the prehydrolytic open state (O1) upon ATP binding to the vacant ABP2. Moreover, we also raised the possibility that state X could be a transient open state (Jih et al., 2012). Interestingly, a conservative mutation in NBD1 (W401F, both W and F are aromatic amino acids) can enhance the responsiveness of state X to ATP as well as nonhydrolyzable ATP analogues for reasons yet to be elucidated. Nevertheless, the striking functional similarities between state X in Jih et al. (2012) and the O2 state in this paper prompt us to test the effect of the W401F mutation on R352C-CFTR. Fig. S3 shows a representative single-channel trace of W401F/R352C-CFTR. Compared with R352C-CFTR (Fig. 3), this double mutant also exhibits a preferred order of the gating transition. Quantitative analysis of gating events indeed demonstrates a higher percentage of gating events with reentry transitions in W401F/R352C-CFTR (Table 1).

Kinetics of the O1 and O2 states

We next quantified the kinetics of these two open states by constructing the dwell-time histograms for individual O1 and O2 states as well as for overall open state (O1 + O2). The results reveal that the R352C mutation significantly shortens the total open time (∼150 ms [Fig. S2] vs. ∼400 ms for WT-CFTR ; Vergani et al., 2003; Bompadre et al., 2005a). In addition, the lifetimes of both O1 and O2 states are significantly prolonged by mutating all endogenous cysteine residues (i.e., Cysless). Prolonged O1 and O2 dwell times were also found in W401F/R352C-CFTR, but to a lesser extent. The effect of Cysless and W401F mutations in prolonging the open time of R352C mutant channels is consistent with the observations made for the same mutants in the WT background (Bai et al., 2010; Tsai et al., 2010a).

DISCUSSION

An accidental discovery of the R352C mutation grants us the opportunity to actually "see"—in real time—ATP hydrolysis taking place during CFTR gating as the ordered transition between two distinct levels of open channel conductance (O1 and O2) indicates an input of the free energy from ATP hydrolysis. Based on statistical analyses of this unique gating feature, we conclude that although most of the ATP-induced opening bursts are, as proposed previously (Csanády et al., 2010), strictly coupled to one round of ATP hydrolysis, a considerable amount of opening bursts do entail hydrolysis of more than one ATP molecule. This casual violation of one-to-one stoichiometry is not predicted by previous gating mechanisms; therefore, a revised gating model (Fig. 6) is proposed in an attempt to explain current as well as many previously published results.

Before we discuss this revised gating model and its structure/function implications, we remind our readers that a similarly ordered open-to-open transition, in fact, was first reported in WT-CFTR more than a decade ago (Gunderson and Kopito, 1995). In their heavily filtered (10-Hz) single-channel recordings, Gunderson and Kopito (1995) observed two levels of open-state conductance that appeared mostly in a C→O1→O2→C order in the presence of ATP. After that study, Ishihara and Welsh (1997) showed that the difference in conductance between the O1 and O2 states was caused by a different degree of blockage by the anionic buffer, MOPS, used in the bathing solution. After we made our discovery with R352C-CFTR, we recorded WT-CFTR under conditions described in these early reports, but did

not observe two levels of open channel current. Further studies are needed to uncover the causes of such discrepancy. Nonetheless, the mutant R352C does offer the advantage of observing transitions between the O1 and O2 states with a much better temporal resolution necessary for a more thorough microscopic kinetic analysis.

Kinetic studies of CFTR gating is challenging because of the small conductance of this channel (~10 pS). Fortunately, because CFTR gating transitions are relatively slow (gating cycle = ~1–2 s^{-1}), it is a common practice in the field to apply a low bandwidth filtering (≤100 Hz) for better signal-to-noise ratio (Gunderson and Kopito, 1995; Csanády, 2000, 2010; Ostedgaard et al., 2001; Aleksandrov et al., 2002; Bompadre et al., 2005a,b; Vergani et al., 2005; Tsai et al., 2009). This technical constraint inevitably limits the temporal resolution of our data, as some short-lived events are eliminated by filtering. Thus, we cannot exclude the possibility that very brief closings exist between O1→O2 or O2→O1 transition. Indeed, in the traces presented here, some brief closures were observed within the opening bursts. However, as elaborated in Results, we can be quite certain that these short-lived closed events are different from the closed state C in Scheme 1 because the lifetime of state C is nearly 1 s for R352C-CFTR. Brief intraburst closures, known as flicker closings (C_f), were well characterized in Bompadre et al. (2005b). This short-lived closed state with a lifetime of ~20 ms buried in the opening bursts does not respond to ATP because it is present in the complete absence of ATP. The possibility that state C_f exists in the O2→O1 transition is very low for two reasons. First, our data suggest that this transition is ATP dependent, as more reentry events occur at a higher [ATP] (Table 1), whereas the C_f state does not respond to ATP. Second, with a 100-Hz filtering, the chance that each time we missed an event with a time constant of 20 ms is ~0.2. However, taking traces 2 and 4 in Fig. 5 A as examples, we can derive the probability that every one of the four O2→O1 transitions observed actually contains a flickery closing right before reentry into the O1 state that will be $<(0.2)^4$. For the trace presented in Fig. 5 B, the probability that we have missed such brief closures in five consecutive O2→O1 transitions will be <0.001. Therefore, if a closed state does exist before the O2 state reenters the O1 state, its lifetime has to be much shorter than that of the flicker closings so that it is constantly missed in our recordings. As mentioned in Results, one can always add more states to explain kinetic data, but, at this juncture, we contend that Scheme 2 is the most economical model.

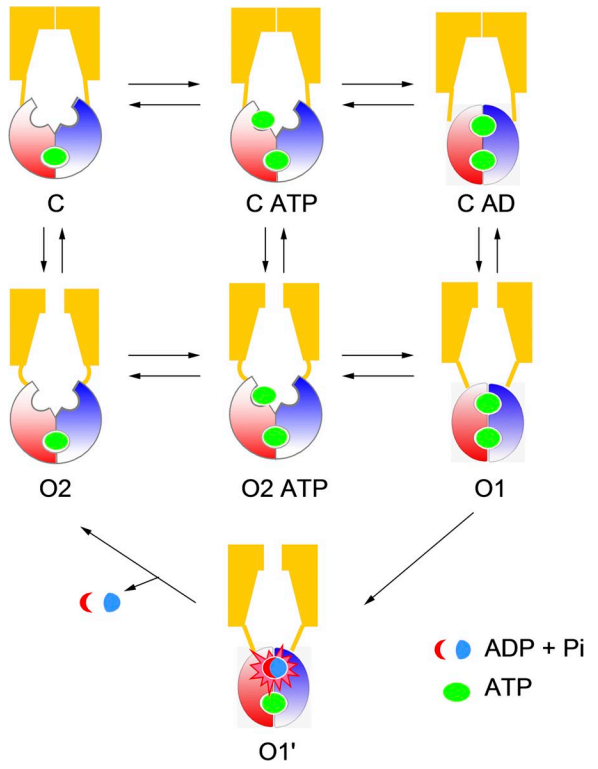

Figure 6. Energetic coupling model for CFTR gating. ATP hydrolysis provides a shortcut from the O1 to O2 state. The C, O1, O2, and O2 ATP states are the same as described in Scheme 2. The O1′ state is added to represent ATP hydrolysis. The C ATP state is added to represent ATP binding before NBD dimerization. The reason for adding the C AD state is described in Discussion.

New insights to the CFTR gating model

With aforementioned caveats in mind, we now expand the simple four-state gating scheme (Scheme 2) and discuss the structure/function implications of a revised gating model. Here, by appending three additional states—two implicitly embedded in the transitions and the other more speculative and supported by previous studies as well as data presented below—we propose a gating model, which is nearly as concise as Scheme 2 but more comprehensible and can potentially bring some fresh insights into the structural mechanism of CFTR gating (Fig. 6).

Upon construction of this model, we incorporated two generally accepted views on CFTR gating: gate opening is triggered by ATP-induced NBD dimerization, and ATP hydrolysis in ABP2 leads to a partial separation of the NBD dimer and closes the gate (Vergani et al., 2005; Csanády et al., 2010; Tsai et al., 2010b). The basic framework of this model is composed of three experimentally detectable states, namely the C, O1, and O2 states, as well as the transitions between them as described above. We reasoned that any ligand-induced conformational changes likely consist of at least two steps: ligand binding and subsequent conformational change. Therefore, for each ATP-dependent transition, C→O1 and O2→O1 in Scheme 2, it is justifiable to insert at least one additional state in between to represent the ATP-bound states, C ATP and O2 ATP. Because ATP hydrolysis is associated with the O1→O2 transition,

we added a transition state simply to depict ATP hydrolysis, a unique feature in CFTR gating. As for the speculative C ATP dimer state (simplified as C AD in Fig. 6) at the top right of the model, there is really no direct evidence establishing its existence because this putative state is a silent state (it does not give out current), and its ATP-binding sites are inaccessible to probes such as nucleotide analogues (Tsai et al., 2009, 2010b; Jih et al., 2012). Thus, its existence can only be inferred. Indeed, through thermodynamic analyses of CFTR gating, Csanády et al. (2006) proposed that NBD dimerization occurs before gate opening. Next, as our data show that binding of a second ATP can occur before gate closure (O2→C), indicating that the NBD dimer is already separated at least partially before the gate closes, it seems unlikely that opening of the gate and formation of the NBD dimer have to be synchronized during the opening process. Furthermore, adding this closed state into the model pleasingly explains some microscopic and macroscopic kinetic data presented below.

The idea that the opening of CFTR by ATP involves three distinct steps—ATP binding (C→CATP), NBD dimerization (CATP→CAD), and gate opening (CAD→O1)—predicts that mutations that disrupt either of these processes can decrease the apparent opening rate. Indeed, mutations of the amino acid residue that directly interacts with ATP have been reported to decrease the opening rate in an ATP-dependent manner (Zhou et al., 2006); further, mutations located at the NBD dimer interface have also been shown to lower the opening rate (e.g., T1246N in Vergani et al., 2005). Here, we show that mutating R352 leads to a reduced opening rate (1 s^{-1} for R352C-CFTR vs. 2.5 s^{-1} for WT-CFTR; Vergani et al., 2003; Bompadre et al., 2005a). Because the R352 residue, located in TMDs, is unlikely to be involved directly in ATP binding or in NBD dimerization, we reckoned mutations at this position could decrease the apparent opening rate by affecting the CAD→O1 transition, a step expected to take place in CFTR's TMDs. Kinetically, the presence of the CAD state also dictates that the gate can close, probably very briefly, even if the NBD dimer has not separated yet (i.e., O1→CAD). These events reflecting channel shuttling between O1 and C AD, if they exist, should be embedded in an opening burst. However, "seeing" these events will be challenging, as they are likely to be masked by the great number of intraburst voltage-dependent flickery closures, some of which are probably caused by a pore-blocking mechanism (Zhou et al., 2001) and are normally eliminated by various means during kinetic analysis to extract ATP-dependent events (Csanády, 2000; Bompadre et al., 2005b). Consistent with this idea, however, previous studies (Bompadre et al., 2005b) did identify two distinguishable populations of intraburst closed events embedded in a long opening burst of a hydrolysis-deficient mutant CFTR. It would be interesting to find out in the future whether these transitions may signify events other than simple channel blockade.

The three-step opening process described above also means that the closing of the hydrolysis-deficient CFTR mutant channels upon removal of ATP will go through three reverse steps: O1→CAD, CAD→CATP, and CATP→C. Because in the absence of ATP hydrolysis the O1→O2 ATP rate is very slow (the gating constant of the O1↔O2 ATP transition is <0.0005; see supplemental Discussion for elaboration), the closing of hydrolytic-deficient channels would not go through a

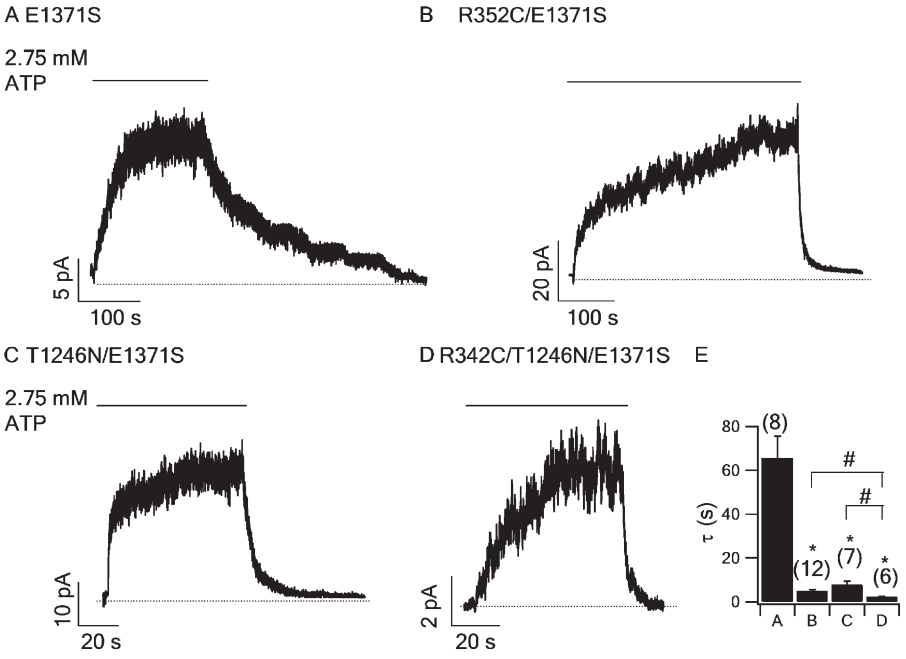

Figure 7. R352C shorten the locked-open time of hydrolytic-deficient CFTR mutant. Macroscopic current traces of E1371S-CFTR (A), R352C/E1371S-CFTR (B), T1246N/E1371S-CFTR (C), and R352C/T1246N/E1371S-CFTR (D). In each panel, the current was activated by PKA + ATP to a steady state, and then PKA and ATP were removed to allow the current to decay. The current relaxation was fitted with a single-exponential function resulting in the relaxation time constant for each mutant: 65.6 ± 10.1 s (n = 8) for E1371S-CFTR, 4.9 ± 0.8 s (n = 12) for R352C/E1371S-CFTR, 7.8 ± 1.6 s (n = 7) for T1246N/E1371S-CFTR, and 2.27 ± 0.27 s (n = 6) for R352C/T1246N/E1371S-CFTR. (E) Bar chart summarizing the results in A–D. *, P < 0.05 compared with E1371S; #, P < 0.05 between two designated data.

O1→O2 ATP→O2→C pathway. It follows that mutations that decrease the rate of NBD dimerization (CATP→CAD), e.g., T1246N in Vergani et al. (2005), or those that reduce the rate for CAD→O1 (presumably the R352C mutation), will accelerate the decay rate of macroscopic currents in hydrolysis-deficient mutants upon ATP washout. Here, in Fig. 7, we show that both R352C and T1246N mutations significantly shorten the locked-open time of the hydrolytic-deficient E1371S-CFTR (Fig. 7). Notably, this result is somewhat different from that shown in Vergani et al. (2005) in which the current relaxation is prolonged in T1246N/K1250R-CFTR. Further studies are required to investigate the functional role of T1246 residue in detail. Nonetheless, the locked-open time is further shortened when combining R352C and T1246N mutations together (Fig. 7, D and E), suggesting that the two mutations affects two different kinetic steps as described above.

Functional implications of the revised gating model

One appealing feature of the proposed model is its symmetry when the hydrolysis pathway is taken away. The whole scheme is then divided into three reversible processes: ligand binding/unbinding (first horizontal transitions), NBD association/dissociation (second horizontal transitions), and gate opening/closing (three vertical transitions). One thermodynamic outcome from this equilibrium scheme is the conclusion that the states harboring an NBD dimer (O1 and CAD) are most energetically stable in the presence of ATP. (See supplemental Discussion for a more comprehensive elaboration.) Thus, ATP hydrolysis simply provides a shortcut for the channel to rapidly escape the absorbing states to carry on the gating cycle.

By assigning NBD dimerization and gate opening as two distinct steps, this model also explicitly states that they are energetically coupled: NBD dimerization favors gate opening and vice versa. This interpretation then distinguishes CFTR from other conventional ligand-gated channels, which couple the ligand-binding energy to the gating conformational change. Instead, CFTR operates as an NBD dimerization-gated channel, although the fundamental principle is the same (Monod et al., 1965). CFTR appears like a ligand-gated channel simply because ATP binding accelerates the dimerization process. It is therefore not surprising that mutations that facilitate the formation of the NBD dimer also promote gate opening even in the absence of ATP (Szollosi et al., 2010). Furthermore, when two NBDs are cross-linked to form a head-to-tail dimer, macroscopic fluctuations reflecting opening and closing of the gate can be discerned in ATP-independent currents (Mense et al., 2006).

Besides shedding light on the coupling mechanism of CFTR gating, the hydrolysis-dependent O1→O2 transition also bears some implications on the TMD configuration during gating. The difference in conductance between the O1 and O2 states indicates a conformational difference between these two states. Thus, the motions of the TMDs are not limited to opening/closing of the gate, as demonstrated previously (Bai et al., 2010, 2011); some structural changes of the pore have occurred after ATP hydrolysis despite the fact that the gate remains open. The molecular basis of such conformational change is unclear and requires further studies.

In conclusion, capitalizing on the unique gating features of R352C-CFTR, we were able to visualize ATP hydrolysis in real time for CFTR by simply monitoring single-channel current traces. We found a nonintegral stoichiometry between the ATP hydrolysis cycle and the gating cycle. Based on this finding, we proposed a gating model that features an energetic coupling between CFTR's NBDs and the TMDs. It would certainly be interesting to see if such a mechanism can be generalized for other ABC transporters.

We thank Dr. Min Li and Cindy Chu for technical assistance. We also thank the editor for his help in trimming our Discussion.

This work was supported by National Institutes of Health (grant R01DK55835) and a grant (Hwang11P0) from the Cystic Fibrosis Foundation to T.-C. Hwang, and by KAKENHI (JSPS22590212 and MEXT23118714) and Keio Gijuku Academic Development Funds to Y. Sohma.

Christopher Miller served as editor.

Submitted: 17 May 2012
Accepted: 17 August 2012

REFERENCES

Aleksandrov, A.A., L. Aleksandrov, and J.R. Riordan. 2002. Nucleoside triphosphate pentose ring impact on CFTR gating and hydrolysis. *FEBS Lett.* 518:183–188. http://dx.doi.org/10.1016/S0014-5793(02)02698-4

Aller, S.G., J. Yu, A. Ward, Y. Weng, S. Chittaboina, R. Zhuo, P.M. Harrell, Y.T. Trinh, Q. Zhang, I.L. Urbatsch, and G. Chang. 2009. Structure of P-glycoprotein reveals a molecular basis for poly-specific drug binding. *Science.* 323:1718–1722. http://dx.doi.org/10.1126/science.1168750

Bai, Y., M. Li, and T.C. Hwang. 2010. Dual roles of the sixth transmembrane segment of the CFTR chloride channel in gating and permeation. *J. Gen. Physiol.* 136:293–309. http://dx.doi.org/10.1085/jgp.201010480

Bai, Y., M. Li, and T.C. Hwang. 2011. Structural basis for the channel function of a degraded ABC transporter, CFTR (ABCC7). *J. Gen. Physiol.* 138:495–507. http://dx.doi.org/10.1085/jgp.201110705

Bompadre, S.G., T. Ai, J.H. Cho, X. Wang, Y. Sohma, M. Li, and T.C. Hwang. 2005a. CFTR gating I: Characterization of the ATP-dependent gating of a phosphorylation-independent CFTR channel (ΔR-CFTR). *J. Gen. Physiol.* 125:361–375. http://dx.doi.org/10.1085/jgp.200409227

Bompadre, S.G., J.H. Cho, X. Wang, X. Zou, Y. Sohma, M. Li, and T.C. Hwang. 2005b. CFTR gating II: Effects of nucleotide binding on the stability of open states. *J. Gen. Physiol.* 125:377–394. http://dx.doi.org/10.1085/jgp.200409228

Carson, M.R., S.M. Travis, and M.J. Welsh. 1995. The two nucleotide-binding domains of cystic fibrosis transmembrane conductance regulator (CFTR) have distinct functions in controlling channel activity. *J. Biol. Chem.* 270:1711–1717. http://dx.doi.org/10.1074/jbc.270.4.1711

Csanády, L. 2000. Rapid kinetic analysis of multichannel records by a simultaneous fit to all dwell-time histograms. *Biophys. J.* 78:785–799. http://dx.doi.org/10.1016/S0006-3495(00)76636-7

Csanády, L., D. Seto-Young, K.W. Chan, C. Cenciarelli, B.B. Angel, J. Qin, D.T. McLachlin, A.N. Krutchinsky, B.T. Chait, A.C. Nairn, and D.C. Gadsby. 2005. Preferential phosphorylation of R-domain serine 768 dampens activation of CFTR channels by PKA. *J. Gen. Physiol.* 125:171–186. http://dx.doi.org/10.1085/jgp.200409076

Csanády, L., A.C. Nairn, and D.C. Gadsby. 2006. Thermodynamics of CFTR channel gating: a spreading conformational change initiates an irreversible gating cycle. *J. Gen. Physiol.* 128:523–533. http://dx.doi.org/10.1085/jgp.200609558

Csanády, L., P. Vergani, and D.C. Gadsby. 2010. Strict coupling between CFTR's catalytic cycle and gating of its Cl- ion pore revealed by distributions of open channel burst durations. *Proc. Natl. Acad. Sci. USA.* 107:1241–1246. http://dx.doi.org/10.1073/pnas.0911061107

Cui, G., Z.R. Zhang, A.R. O'Brien, B. Song, and N.A. McCarty. 2008. Mutations at arginine 352 alter the pore architecture of CFTR. *J. Membr. Biol.* 222:91–106. http://dx.doi.org/10.1007/s00232-008-9105-9

Dawson, R.J., and K.P. Locher. 2006. Structure of a bacterial multidrug ABC transporter. *Nature.* 443:180–185. http://dx.doi.org/10.1038/nature05155

Gadsby, D.C., T.C. Hwang, T. Baukrowitz, G. Nagel, M. Horie, and A.C. Nairn. 1994. Regulation of CFTR channel gating. *Jpn. J. Physiol.* 44:S183–S192.

Gaudet, R., and D.C. Wiley. 2001. Structure of the ABC ATPase domain of human TAP1, the transporter associated with antigen processing. *EMBO J.* 20:4964–4972. http://dx.doi.org/10.1093/emboj/20.17.4964

Gunderson, K.L., and R.R. Kopito. 1994. Effects of pyrophosphate and nucleotide analogs suggest a role for ATP hydrolysis in cystic fibrosis transmembrane regulator channel gating. *J. Biol. Chem.* 269:19349–19353.

Gunderson, K.L., and R.R. Kopito. 1995. Conformational states of CFTR associated with channel gating: the role ATP binding and hydrolysis. *Cell.* 82:231–239. http://dx.doi.org/10.1016/0092-8674(95)90310-0

Hollenstein, K., D.C. Frei, and K.P. Locher. 2007. Structure of an ABC transporter in complex with its binding protein. *Nature.* 446:213–216. http://dx.doi.org/10.1038/nature05626

Hwang, T.C., G. Nagel, A.C. Nairn, and D.C. Gadsby. 1994. Regulation of the gating of cystic fibrosis transmembrane conductance regulator C1 channels by phosphorylation and ATP hydrolysis. *Proc. Natl. Acad. Sci. USA.* 91:4698–4702. http://dx.doi.org/10.1073/pnas.91.11.4698

Ishihara, H., and M.J. Welsh. 1997. Block by MOPS reveals a conformation change in the CFTR pore produced by ATP hydrolysis. *Am. J. Physiol.* 273:C1278–C1289.

Ivetac, A., J.D. Campbell, and M.S. Sansom. 2007. Dynamics and function in a bacterial ABC transporter: simulation studies of the BtuCDF system and its components. *Biochemistry.* 46:2767–2778. http://dx.doi.org/10.1021/bi0622571

Jih, K.Y., Y. Sohma, M. Li, and T.C. Hwang. 2012. Identification of a novel post-hydrolytic state in CFTR gating. *J. Gen. Physiol.* 139:359–370. http://dx.doi.org/10.1085/jgp.201210789

Karpowich, N., O. Martsinkevich, L. Millen, Y.R. Yuan, P.L. Dai, K. MacVey, P.J. Thomas, and J.F. Hunt. 2001. Crystal structures of the MJ1267 ATP binding cassette reveal an induced-fit effect at the ATPase active site of an ABC transporter. *Structure.* 9:571–586. http://dx.doi.org/10.1016/S0969-2126(01)00617-7

Khare, D., M.L. Oldham, C. Orelle, A.L. Davidson, and J. Chen. 2009. Alternating access in maltose transporter mediated by rigid-body rotations. *Mol. Cell.* 33:528–536. http://dx.doi.org/10.1016/j.molcel.2009.01.035

Kopeikin, Z., Y. Sohma, M. Li, and T.C. Hwang. 2010. On the mechanism of CFTR inhibition by a thiazolidinone derivative. *J. Gen. Physiol.* 136:659–671. http://dx.doi.org/10.1085/jgp.201010518

Lewis, H.A., S.G. Buchanan, S.K. Burley, K. Conners, M. Dickey, M. Dorwart, R. Fowler, X. Gao, W.B. Guggino, W.A. Hendrickson, et al. 2004. Structure of nucleotide-binding domain 1 of the cystic fibrosis transmembrane conductance regulator. *EMBO J.* 23:282–293. http://dx.doi.org/10.1038/sj.emboj.7600040

Mense, M., P. Vergani, D.M. White, G. Altberg, A.C. Nairn, and D.C. Gadsby. 2006. In vivo phosphorylation of CFTR promotes formation of a nucleotide-binding domain heterodimer. *EMBO J.* 25:4728–4739. http://dx.doi.org/10.1038/sj.emboj.7601373

Monod, J., J. Wyman, and J.P. Changeux. 1965. On the nature of allosteric transitions: a plausible model. *J. Mol. Biol.* 12:88–118. http://dx.doi.org/10.1016/S0022-2836(65)80285-6

Ostedgaard, L.S., O. Baldursson, and M.J. Welsh. 2001. Regulation of the cystic fibrosis transmembrane conductance regulator Cl-channel by its R domain. *J. Biol. Chem.* 276:7689–7692. http://dx.doi.org/10.1074/jbc.R100001200

Richard, E.A., and C. Miller. 1990. Steady-state coupling of ion-channel conformations to a transmembrane ion gradient. *Science.* 247:1208–1210. http://dx.doi.org/10.1126/science.2156338

Szollosi, A., P. Vergani, and L. Csanády. 2010. Involvement of F1296 and N1303 of CFTR in induced-fit conformational change in response to ATP binding at NBD2. *J. Gen. Physiol.* 136:407–423. http://dx.doi.org/10.1085/jgp.201010434

Szollosi, A., D.R. Muallem, L. Csanády, and P. Vergani. 2011. Mutant cycles at CFTR's non-canonical ATP-binding site support little interface separation during gating. *J. Gen. Physiol.* 137:549–562. http://dx.doi.org/10.1085/jgp.201110608

Tsai, M.F., H. Shimizu, Y. Sohma, M. Li, and T.C. Hwang. 2009. State-dependent modulation of CFTR gating by pyrophosphate. *J. Gen. Physiol.* 133:405–419. http://dx.doi.org/10.1085/jgp.200810186

Tsai, M.F., K.Y. Jih, H. Shimizu, M. Li, and T.C. Hwang. 2010a. Optimization of the degenerated interfacial ATP binding site improves the function of disease-related mutant cystic fibrosis transmembrane conductance regulator (CFTR) channels. *J. Biol. Chem.* 285:37663–37671. http://dx.doi.org/10.1074/jbc.M110.172817

Tsai, M.F., M. Li, and T.C. Hwang. 2010b. Stable ATP binding mediated by a partial NBD dimer of the CFTR chloride channel. *J. Gen. Physiol.* 135:399–414. http://dx.doi.org/10.1085/jgp.201010399

Vergani, P., A.C. Nairn, and D.C. Gadsby. 2003. On the mechanism of MgATP-dependent gating of CFTR Cl^- channels. *J. Gen. Physiol.* 121:17–36. http://dx.doi.org/10.1085/jgp.20028673

Vergani, P., S.W. Lockless, A.C. Nairn, and D.C. Gadsby. 2005. CFTR channel opening by ATP-driven tight dimerization of its nucleotide-binding domains. *Nature.* 433:876–880. http://dx.doi.org/10.1038/nature03313

Zhou, Z., S. Hu, and T.C. Hwang. 2001. Voltage-dependent flickery block of an open cystic fibrosis transmembrane conductance regulator (CFTR) channel pore. *J. Physiol.* 532:435–448. http://dx.doi.org/10.1111/j.1469-7793.2001.0435f.x

Zhou, Z., X. Wang, H.Y. Liu, X. Zou, M. Li, and T.C. Hwang. 2006. The two ATP binding sites of cystic fibrosis transmembrane conductance regulator (CFTR) play distinct roles in gating kinetics and energetics. *J. Gen. Physiol.* 128:413–422. http://dx.doi.org/10.1085/jgp.200609622